Refraction of Diffuse Photon Density Waves

M. A. O'Leary,[1,2] D. A. Boas,[1,2] B. Chance,[2] and A. G. Yodh[1]

[1]*Department of Physics, University of Pennsylvania, Philadelphia, Pennsylvania 19104-6396*

[2]*Department of Biochemistry and Biophysics, University of Pennsylvania, Philadelphia, Pennsylvania 19104-6089*

(Received 10 August 1992)

Experiments are performed which illustrate the properties of damped traveling waves in diffusive media. Our observations demonstrate the manipulation of these waves by adjustment of the photon diffusion coefficients of adjacent turbid media. The waves are imaged, and are shown to obey simple relations such as Snell's law. The extent to which analogies from physical optics may be used to understand these waves is further explored, and the implications for medical imaging are briefly discussed.

PACS numbers: 42.25.Gy, 41.20.Jb, 42.25.Md, 42.62.Be

The correlation and transport properties of diffuse light have been the subject of intense recent interest [1]. A practical aspect of these problems concerns the potential uses of diffuse light to locate objects embedded within turbid media [2]. By turbid media, we mean any medium in which the transport of light energy density, $U(\mathbf{r},t)$, is governed by the diffusion equation [3], $\partial U/\partial t = D\nabla^2 U$. To this end a variety of probes, including amplitude modulated (AM) continuous-wave laser sources [4], have been employed to study the effects of inhomogeneities on optical path lengths in model biological systems. Interestingly, insertion of the AM light source into any optically dense random medium is accompanied by the generation of a small but measurable traveling wave disturbance of the light energy density which we will hereafter refer to as a *diffuse photon density wave.*

Diffuse photon density waves are scalar, damped, traveling waves. These highly damped traveling waves arise formally in *any* diffusive system that is driven by an oscillating source [5]. Recently the problem has been discussed within the context of diffuse photon transport [6-8]. Fishkin and Gratton, for example [8], have calculated the light energy density, $U(\mathbf{r},t)$, within an optically dense homogeneous media in the presence of a modulated point light source at the origin. They then used the result and the principle of superposition to derive the light energy density in the presence of an absorbing semi-infinite plane. The oscillatory part of the solution for an *infinite*, homogeneous, nonabsorbing dense random media is [6,8]

$$U_{\mathrm{ac}}(\mathbf{r},t) = (A/Dr)\exp\{-k\cos\varphi r\} \times \exp\{ik\sin\varphi r - i\omega t\}\,, \quad (1)$$

where A is a constant, $D = \frac{1}{3}(c/n)l^*$ is the diffusion coefficient for light in the media, l^* is the photon transport mean free path in the medium, c/n is the speed of light in the medium, ω is the source modulation frequency, and in the absence of absorption [9] $\varphi = \pi/4$ and $k = (\omega/D)^{1/2}$. Although the wave is very rapidly attenuated, it has a well-defined wavelength, amplitude, and phase at all points. Qualitatively, this wavelength corresponds to the root-mean-square displacement experienced by a typical photon during a single modulation period. It can be altered by modifying D or ω.

In this paper we inquire further into the basic properties of these waves. We present experimental observations of circular wave fronts and we examine how these wave fronts propagate from one semi-infinite turbid media to another. Our results *experimentally* demonstrate that a "diffusional index of refraction" is a useful concept for these waves, and that it is possible to manipulate them by controlling the *photon diffusion coefficients* (D) of adjacent turbid media. This may be of considerable importance in biological systems, where the natural curvature of organs such as the brain, heart, or kidney, together with changes of scattering and absorption as in the grey-white matter transition of the brain, can lead to significant modifications of the trajectories of diffuse photons. While the potential for focusing has been noted qualitatively in one early paper [6], to our knowledge the present observations are the first documented experiments of refraction phenomena in a diffusive system. We also discuss briefly the extent to which simple ideas from physical optics, such as Huygen's principle, might be adapted to better understand phase images that can be formed using these waves.

The experimental apparatus is depicted in Fig. 1. The dense random medium we used was a liquid called Intralipid [10]. Intralipid is a polydisperse suspension of particles with an average diameter of ~ 0.4 μm, but a relatively wide range of sizes (i.e., from ~ 0.1 to ~ 1.1 μm). By changing the solution concentration we were able to vary the light diffusion coefficient of the medium. The photon transport mean free path l^* was about 0.2 cm in a 0.5% concentrated solution. Typically we filled a large fish tank (30 cm $\times$ 30 cm $\times$ 60 cm) with Intralipid. We performed experiments in three geometries. In the first case there was no partition and the sample was homogeneous. In the other two cases, a plane or cylindrical acrylic partition separated two solutions with different concentrations. In our experiments the absorption is very small, the suspensions are dilute, and therefore the diffusion coefficient is inversely proportional to the Intralipid concentration.

Source and detector optical fibers (~ 4 mm in diameter) were immersed in the solution at the same height

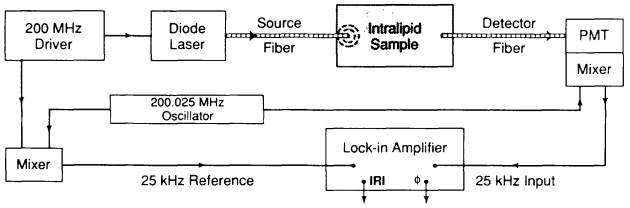

FIG. 1. A known concentration of Intralipid sample fills a glass fish tank. Our source is a diode laser that is amplitude modulated by a 200-MHz driver. Light is delivered into the sample through a source fiber, and picked up by a movable detector fiber. The fibers are pointed in orthogonal directions to minimize gradient systematics. The signal at the photomultiplier tube (PMT) is down-converted to 25 kHz (by modulating a PMT dynode at 200.025 MHz), and then fed into a lock-in amplifier. The 25-kHz lock-in reference signal is derived from the 200-MHz driver by standard mixing techniques. The two-phase lock-in provides amplitude ($|\mathbf{R}|$), and phase (ϕ) output signals.

above the tank floor. The source light was derived from a 3-mW diode laser operating at 816 nm. The diode laser was amplitude modulated at 200 MHz, and the source fiber position was fixed. The detector fiber could be positioned anywhere in the plane, and was connected to a photomultiplier tube on its other end. In order to facilitate the phase and amplitude measurements, both the reference signal from the source and the detected signal were down-converted to 25 kHz by heterodyning with a second oscillator at 200.025 MHz. The low-frequency signals were then measured using a lock-in amplifier. The phase shift (and ac amplitude) of the detected light was measured with respect to the source at each point on a 0.5-cm square planar grid throughout the sample. Constant phase contours were easily determined by linear interpolation of the grid data. The sensitivity of our current apparatus is about 10^5. Since the signal amplitude decays by $> e^{-2\pi}$ in one wavelength, the range of our experiments is limited to slightly more than one wavelength. Nevertheless, it is possible to clearly distinguish the essential physical phenomena in the present experiments.

Our results for the $\sim$0.5% concentrated homogeneous media are exhibited in Fig. 2. Constant phase contours are shown at 20° intervals about the source in Fig. 2. Notice that the contours are circular, and that their radii can be extrapolated back to the source. In the inset of Fig. 2 we plot the phase shift and the quantity $\ln|rU_{ac}(\mathbf{r},t)|$ as a function of radial distance from the source. From these measurements we deduce the wavelength of the diffuse photon density wave (11.2 cm), as well as the photon transport mean free path ($\sim$0.2 cm), and the photon absorption length ($\sim$52 cm) [9] in $\sim$0.5% Intralipid at 22 °C. The photon absorption can be attributed almost entirely to water [11].

In Fig. 3 we demonstrate the refraction of these waves

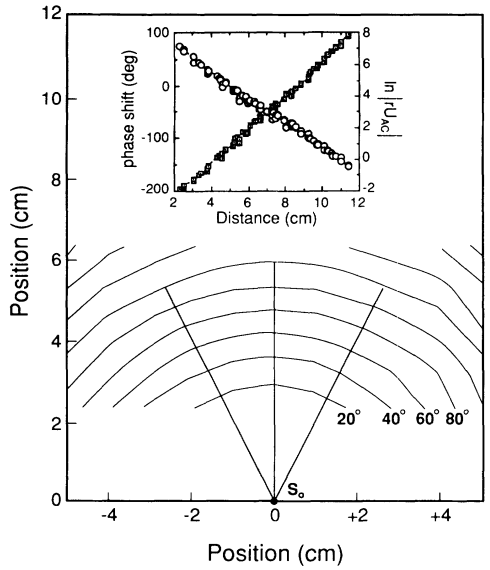

FIG. 2. Constant phase contours shown as a function of position for homogeneous, 0.5% Intralipid solution. The contours are shown in 20° intervals. Inset: The measured phase shift (circles) and $\ln|rU_{ac}(\mathbf{r},t)|$ (squares) are plotted as a function of radial distance from the source S_o.

in three ways. Figure 3 shows constant phase contours (every 20°). This time, however, a plane boundary is introduced separating the lower medium with concentration $c_l \approx 1.0\%$ and light diffusion coefficient D_l from the upper medium with concentration $c_u \approx 0.25\%$ and light diffusion coefficient D_u. The contours below the boundary are just the homogeneous media contours (without

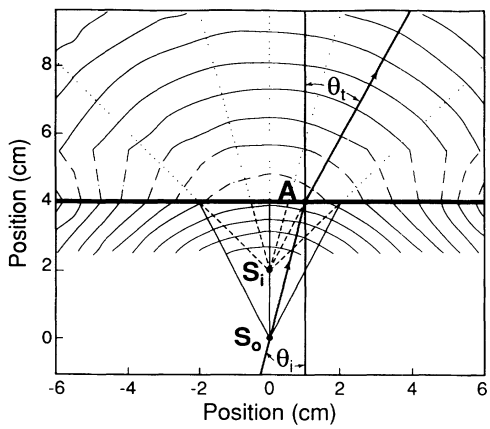

FIG. 3. Constant phase contours (in 20° intervals) as a function of position showing the propagation of a diffuse photon density wave across a planar boundary that separates 1% concentrated Intralipid from 0.25% Intralipid. See text for detailed discussion. S_o, source position; S_i, apparent source position; A, point on boundary; θ_i, angle of incident ray; θ_t, angle of refracted ray. The solid lines are obtained directly from data. The dot-dashed lines are obtained by interpolation over large distances, and are drawn to show the irregularities at large angles.

reflection); they are obtained *before* the partition is introduced into the sample. The contours above the boundary are derived from the diffuse photon density waves transmitted into the less concentrated medium. As a result of our detector geometry, our closest approach to the partition was about 1 cm. We expect a number of general results. First, the wavelength in the less dense medium ($\lambda_u = 14.8$ cm) should be greater than the wavelength of the diffuse photon density wave in the incident medium ($\lambda_l = 8.17$ cm). This was observed. The ratio of the two wavelengths should equal the ratio of the diffusional indices of refraction of the two media. Specifically we found, as expected, that $\lambda_u = \lambda_l (D_l/D_u)^{-1/2} \sim \lambda_l (c_l/c_u)^{1/2}$. Furthermore, we would expect that the apparent source position (S_i), *as viewed from within the upper medium*, should be shifted from the real source position ($S_o = 4.0 \pm 0.2$ cm) by a factor $\lambda_l/\lambda_u = 0.55$. Within the accuracy of this measurement this is what we find. Using the radii from the full contour plots we see that the apparent source position is shifted from 4.0 ± 0.2 to 2.0 ± 0.25 cm.

Finally in Fig. 3 we explicitly demonstrate Snell's law for diffuse photon density waves. This can be seen by following the ray from S_o to the point A at the boundary, and then into the upper medium. The ray in the lower medium makes an angle $\theta_i = 14°$ with respect to the surface normal. The upper ray is constructed in the standard way between the apparent source position S_i, through the point A on the boundary, and into the medium above the boundary [12]. It is perpendicular to the circular wave fronts in the less dense medium, and makes an angle $\theta_t = 26.6°$ with respect to the boundary normal. Within the accuracy of the experiment we see that $\sin\theta_i/\sin\theta_t = 0.54 \approx \lambda_l/\lambda_u$, so that Snell's law accurately describes the propagation of diffuse photon density waves across the boundary. It is interesting to note that the wave fronts become quite distorted when the source ray angle exceeds $\sim 30°$. These irregularities are a consequence of total internal reflection, diffraction, and some spurious boundary effects. We will discuss the phenomena in greater detail in a future paper.

A third important observation we make in this work is presented in Fig. 4. Here we use a circular boundary separating two turbid media to demonstrate that we can alter the curvature of the diffuse photon density wave fronts in analogy with a simple lens in optics. Again two semi-infinite media are separated by a boundary. This time the medium on the right is more concentrated. The constant phase contours of the transmitted wave exhibit a shorter wavelength, and are clearly converging toward some image point to the right of the boundary. The medium on the left (λ_l) has an Intralipid concentration of $\sim 0.1\%$, and the medium on the right (λ_r) has a concentration of $\sim 1.6\%$, and the wavelength ratio was measured to be $\lambda_r/\lambda_l = 3.8 \pm 0.3$. The curved surface has a radius $R = 9.0 \pm 0.4$ cm. The object position (the source) is $S_o = 9.4 \pm 0.3$ cm. The image position was determined

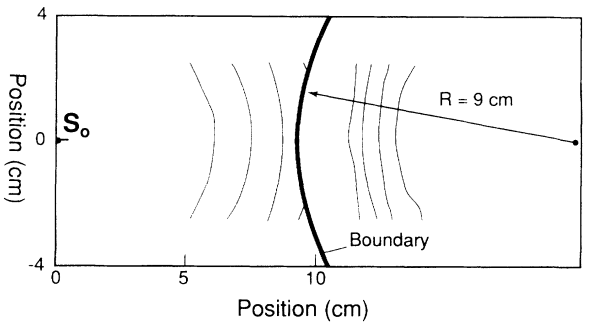

FIG. 4. Refraction by a spherical surface. A curved boundary separates two media of different concentration, and modifies the curvature of an incident diffuse photon density wave. The constant phase contours on the left occur in 20° intervals, and the constant phase contours on the right occur in 40° intervals. The reversal of wave-front curvature is evident.

to be $S_i = 12 \pm 2$ cm. This result deviates somewhat from the well-known paraxial result from geometrical optics for imaging by a spherical refracting surface [12]. The deviation is primarily a result of spherical aberration [12]. The central point remains, however; that is, the curvature of the wave fronts is reversed after traversing the circular boundary.

The experiments depicted in Figs. 2, 3, and 4 indicate that it is possible to exert substantial control over the transport of diffuse light in dense random media. We have clearly demonstrated that the index of refraction of these waves depends on the photon diffusion coefficient or random walk step in these media. Further work remains, not only with regard to analogous optical effects and quantitation, but towards utilizing these waves to image inhomogeneities within turbid media. Work along these lines is under way in our laboratories. Presently, however, we comment on some important ideas from optics that may be of use in considering the scattering and propagation of these waves. In the following discussion we will *ignore the effects of absorption*, and we will assume that the time it takes for light to travel a single random walk step is much shorter than the modulation period as in these studies.

In deriving Eq. (1) from the differential form of Fick's law and photon flux conservation, one finds that the oscillatory part of the light energy density $U_\omega(\mathbf{r})$ obeys the Helmholtz equation, i.e., $(\nabla^2 + k^2)U_\omega(\mathbf{r}) = 0$. The only significant difference in comparison to conventional wave phenomena is that $k^2 = i(\omega/D)$, and therefore k is complex. The spatial part of $U_{ac}(\mathbf{r},t)$ in Eq. (1) is simply the Green's function solution of the Helmholtz equation with the appropriate k. These similarities suggest that some basic theorems that apply to solutions of the Helmholtz equation will apply to these diffuse photon density waves. For example, one can construct a Kirchhoff integral for these waves [13], using the Green's-function solution. This provides a formal apparatus by which to calculate the wave amplitude and phase at various distances from a

"diffracting" aperture. To the extent that the Kirchhoff integral embodies the basic Huygens-Fresnel principle we may envision the contributions of different elements of a scattering surface as arising from *damped*, spherical point sources. This also implies that the focusing of diffuse photon density waves will have the same limitations due to diffraction as in the case of light.

With further improvements in the signal-to-noise ratio we should be able to increase the range of our measurements to several wavelengths. Unfortunately, we still will not be able to take advantage of many of the far-field results often used in optics. Nevertheless, the near-field form of the solution provides a framework by which we can understand the phase and amplitude images formed by scatterers in dense random media. In practical biomedical scenarios we will be looking for distortions of these wave fronts as a result of absorptive and dispersive inhomogeneities within objects such as the human breast. Since the radius of the human breast is reachable within a range of one wavelength, imaging of small breast tumors appears to be feasible. In the present paper we have taken a first step towards this goal by discerning structure within a two-component sample.

We are happy to acknowledge useful conversations with Peter Kaplan, Charles Kane, Tom Lubensky, Michael Cohen, and Dinos Gonatas, as well as the technical assistance of Jian Weng. A.G.Y. gratefully acknowledges partial support from the National Science Foundation through the Presidential Young Investigator program and Grant No. DMR-9003687, and from the Alfred P. Sloan Foundation. B.C. gratefully acknowledges support from HL-44125, ACSBE-B, NS-27346, and Hamamatsu Photonics.

[1] See, for example, S. John, Phys. Today **44**, No. 5, 32 (1991); S. Feng and P. A. Lee, Science **251**, 633 (1991); D. J. Durian, D. A. Weitz, and D. J. Pine, Science **252**, 686 (1991), and references therein.

[2] See, for example, imaging overviews in *Future Trends in Biomedical Applications of Lasers*, SPIE Proceedings Vol. 1525 (SPIE-International Society for Optical Engineering, Bellingham, WA, 1991).

[3] A. Ishimaru, *Wave Propagation and Scattering in Random Media* (Academic, New York, 1978), Vol. 1.

[4] See, for example, B. J. Tromberg, L. O. Svaasand, T. Tsay, R. C. Haskell, and M. W. Berns, in *Future Trends in Biomedical Applications of Lasers* (Ref. [2]), p. 52, and references therein.

[5] For an interesting example of a diffusion wave in the context of heat conduction, see A. Sommerfeld, *Partial Differential Equations in Physics* (Academic, New York, 1949), p. 68.

[6] E. Gratton, W. Mantulin, M. J. van de Ven, J. Fishkin, M. Maris, and B. Chance, in *Proceedings of the Third International Conference: Peace through Mind/Brain Science, 1990* (Hamamatsu Photonics KK, Hamamatsu, 1990), p. 183.

[7] A. Knuttel, J. M. Schmidt, and J. R. Knudsen, Appl. Opt. (to be published).

[8] J. Fishkin and E. Gratton, J. Opt. Soc. Am. A (to be published).

[9] For a medium characterized by absorption length l_a, $\tan 2\varphi = (\omega l_a)n/c$. Absorptive corrections to k and D are small for the samples we consider, and can be found in [6,8].

[10] The Intralipid used here can be obtained from Kabi Pharmacia in Clayton, North Carolina.

[11] C. M. Hale and M. R. Querry, Appl. Opt. **12**, 555 (1973).

[12] E. Hecht, *Optics* (Addison-Wesley, Reading, MA, 1987), Chaps. 4–6.

[13] M. Born and E. Wolf, *Principles of Optics* (Pergamon, New York, 1980), Chap. 8.

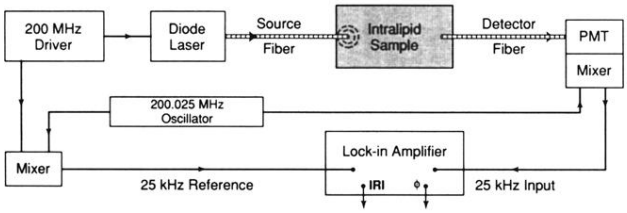

FIG. 1. A known concentration of Intralipid sample fills a glass fish tank. Our source is a diode laser that is amplitude modulated by a 200-MHz driver. Light is delivered into the sample through a source fiber, and picked up by a movable detector fiber. The fibers are pointed in orthogonal directions to minimize gradient systematics. The signal at the photomultiplier tube (PMT) is down-converted to 25 kHz (by modulating a PMT dynode at 200.025 MHz), and then fed into a lock-in amplifier. The 25-kHz lock-in reference signal is derived from the 200-MHz driver by standard mixing techniques. The two-phase lock-in provides amplitude ($|\mathbf{R}|$), and phase (ϕ) output signals.